PB90-263286

Measurement of Aerodynamic Size and Related Risk Assessment of Airborne Fibers

(U.S.) Health Effects Research Lab., Research Triangle Park, NC

1990

U.S. Department of Commerce
National Technical Information Service
NTIS

TECHNICAL REPORT DATA
(Please read Instructions on the reverse before complet

1. REPORT NO.	2.	3. PB90-263286
EPA/600/D-90/130		

4. TITLE AND SUBTITLE	5. REPORT DATE
MEASUREMENT OF AERODYNAMIC SIZE AND RELATED RISK ASSESSMENT OF AIRBORNE FIBERS	6. PERFORMING ORGANIZATION CODE
7. AUTHOR(S) T. MARTONEN	8. PERFORMING ORGANIZATION REPORT NO.
9. PERFORMING ORGANIZATION NAME AND ADDRESS Experimental Dosimetry Branch, ETD Health Effects Research Laboratory, U.S. EPA Research Triangle Park, NC 27711	10. PROGRAM ELEMENT NO. 11. CONTRACT/GRANT NO.
12. SPONSORING AGENCY NAME AND ADDRESS Health Effects Research Laboratory - RTP, NC Office of Research and Development U.S. Environmental Protection Agency Research Triangle Park, NC 27711	13. TYPE OF REPORT AND PERIOD COVERED 14. SPONSORING AGENCY CODE EPA/600/10

15. SUPPLEMENTARY NOTES

16. ABSTRACT

The constituent particles of many ambient and workplace aerosols of health effects concerns are of fibrous and aggregate geometric shapes. The deposition sites of inhaled particles in the human respiratory system are primarily related to their aerodynamic diameters. Therefore, to assess potential exposure hazards it is necessary to have accurate kinetic classifications of airborne particulate matter. A tested theory of operation is given so centrifugal spectrometers can give direct and continuously graded measures of the aerodynamic size distributions of irregular aerosols. Aerosol centrifuge performance therefore can be customized to specific applications and be integrated into health effects studies.

17. KEY WORDS AND DOCUMENT ANALYSIS

a. DESCRIPTORS	b. IDENTIFIERS/OPEN ENDED TERMS	c. COSATI Field/Group

18. DISTRIBUTION STATEMENT	19. SECURITY CLASS *(This Report)*	21. NO. OF PAGES
RELEASE TO THE PUBLIC	UNCLASSIFIED	
	20. SECURITY CLASS *(This page)* UNCLASSIFIED	22. PRICE

EPA Form 2220-1 (Rev. 4-77) PREVIOUS EDITION IS OBSOLETE

PB90-263286

EPA/600/D-90/130

Measurement of Aerodynamic Size and Related Risk Assessment of Airborne Fibers

T.B. Martonen*
Health Effects Research Laboratory
U.S. Environmental Protection Agency
Research Triangle Park, NC 27711

REPRODUCED BY
U.S. DEPARTMENT OF COMMERCE
NATIONAL TECHNICAL
INFORMATION SERVICE
SPRINGFIELD, VA 22161

Summary

The constituent particles of many ambient and workplace aerosols of health effects concerns are of fibrous and aggregate geometric shapes. The deposition sites of inhaled particles in the human respiratory system are primarily related to their aerodynamic diameters. Therefore, to assess potential exposure hazards it is necessary to have accurate kinetic classifications of airborne particulate matter. A tested theory of operation is given so centrifugal spectrometers can give direct and continuously graded measures of the aerodynamic size distributions of irregular aerosols. Aerosol centrifuge performance therefore can be customized to specific applications and be integrated into health effects studies.

1. Introduction

This work addresses the airborne behavior of particulate matter with elongated and/or irregular shapes that are of health effects concerns. Such aerosols include individual fibrous particles, and branching composites created from primary particles of compact geometries. The fibers may be mined minerals or synthetic materials. The latter range from commonly used commercial glass substitutes for asbestos, to metallic and ceramic particles produced in high temperature industrial processes. Examples of the branching arrays are emissions created during the combustion of hydrocarbons, and welding fumes.

A mathematical description of particle behavior in spiral channel centrifuges is presented, and substantiated by comparisons with laboratory calibration data using polystyrene latex spheres. The theory is extended to non-spherical forms by incorporating appropriate dynamic particle shape resistance factors in trajectory equations. It is demonstrated how optimum centrifuge performance is made possible by the *a priori* determination of

favorable operating conditions permitting high-resolution characterization; specifically for fibrous aerosols.

2. Aerosol Dynamics

Deposition efficiencies of particles in the human respiratory tract can be specifically related to the mass median aerodynamic diameter (MMAD) and geometric standard deviation (σ_g) of an inhaled aerosol (Stahlhofen et al. (7)). Therefore, instruments which can directly measure MMAD and σ_g values have immediate applications in risk assessment regimens. Two classes of such devices used in aerosol physics research, and suitable for studying fiber and aggregate behavior are centrifugal spectrometers and cascade impactors. The units give graded measures of the aerodynamic distributions of sampled aerosols. Major advantages of centrifuges over the operation of cascade impactors are: (1) interpretation of size distribution data is not affected by the stage-overlapping of particle deposits, and (2) there are no jet orifices to become clogged by fibers.

2.1 Particle Motion in Airways.

The roles of naturally-occurring and man-made airborne fibers in producing lung fibrosis, cancer and mesothelioma have been well documented, and continue to be foci in health effects studies regarding workplace environments and ambient atmospheres. As noted by Spurny (6) scientific findings "...have convincingly demonstrated the primary importance of fiber geometry on the carcinogenic effect."

The manner in which geometric shapes of fibers affect their trajectories and ultimate sites of deposition within the human respiratory tract is a timely issue. The relatively straight amphilbole and glass particles may align themselves with air streamlines and penetrate to peripheral regions of the lung not anticipated from considerations of physical dimensions only. The splitting, irregular forms of chrysotile however, tend to promote collection on more proximal airway surfaces via a deposition mechanism termed interception. The roles of fiber orientation on deposition in the human respiratory tract were discussed by Harris and Fraser (2). The behavior of inhaled fibers at airway bifurcation sites, clinically known to be locations of enhanced bronchogenic tumors in man, have been experimentally quantitated by Mjoyo (5).

A mathematical model describing the coupled deposition processes of inertial impaction, gravitational settling, and interception at such airway junctures, consistent with Mjoyo's (5) laboratory data, has recently been

derived by Martonen et al. (4). The airborne behavior of fibers in the neighborhood of a lung bifurcation is depicted in Figure 1. The theory clearly demonstrates the importance of particle orientation affecting localized deposition patterns. Predictions of the model emphasize that an accurate aerodynamic characterization of fibers is required to relate their motion and deposition probabilities with dimensions, densities and orientations relative to airstreams.

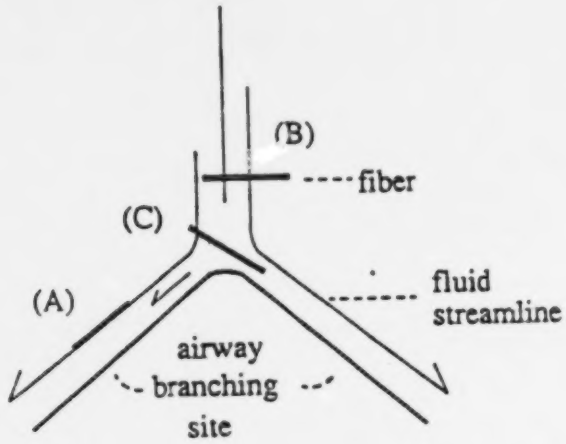

Figure 1. Fiber motion at an airway dividing site. Spatial orientations relative to entraining air streamlines are: (A) parallel, (B) perpendicular, and (C) random.

2.2 Particle Motion in Centrifuges

High resolution aerosol spectrometers, capable of characterizing particles by aerodynamic sizes over two orders of magnitude (e.g., 0.2 - 20 μm) have been developed. Several configurations have been proposed for the geometries of ducts machined into the disc shaped centrifuge rotors. The spiral duct design of Stöber and Flachsbart (8) consists of six offset semicircular turns. In all designs, the aerosol enters at the center of rotation of the rotor, as a thin layer along the inner wall of the duct. Particles are entrained in a laminar stream of clean gas through which they must migrate before being collected along the duct's outer wall. The rate of a particle's movement through this winnowing stream, and therefore its point of deposition on a collection foil, is a function of its aerodynamic diameter.

Consider the motion of a particle moving through a turn of the spiral duct

centrifuge described relative to the (r,θ) cylindrical coordinate system defined in Figure 2. Its origin is the center of curvature of the turn and rotates with uniform angular speed, Ω, the rotating speed of the instrument. The centrifugal and Coriolis acceleration fields acting upon an aerosol particle of mass m are also shown in Figure 2. The centrifugal term due to the rotation of the instrument has a magnitude $\Omega^2 R$ and is directed radially outward from the center of rotation of the instrument. The centrifugal term which results from flow in a curved channel has magnitude $W_\theta{}^2/r$ and is directed radially outward from the center of curvature, as is the Coriolis term of magnitude $2\Omega W_\theta$, where W_θ is the azimuthal component of velocity.

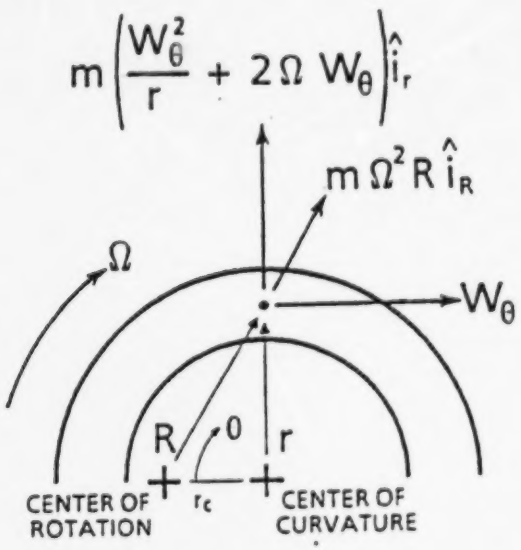

Figure 2. Coriolis and centrifugal force fields acting upon a particle of mass m within a semicircular turn of the spiral duct centrifuge. Unit vectors are denoted by i_r and i_R. There is a constant offset, r_c, and radius of curvature for each semicurcular turn.

Recently, Johnson and Martonen (3) presented general mathematical models of spherical particle behavior, describing size-classifying trajectories in centrifuges. The differential equation which describes particle motion may be expressed as

$$\frac{dr}{d\theta} = \frac{m}{f_d}\left[\left(\frac{\Omega^2}{W_\theta}\right) r^2 + \left(\frac{-\Omega^2 r_c}{W_\theta}\right) r\cos\theta + (2\Omega)\, r\right] \qquad [1]$$

which describes the radial change of position of an aerosol particle as a function of distance down the duct, where $f_d = 3\pi\mu D_g/C(D_g)$ is drag and $C(D_g)$ the slip correction factor. The formulation and solution of the differential equation describing spherical particle kinetics in centrifugal spectrometers has been detailed by Johnson and Martonen (3).

Plots of theoretically predicted versus experimentally observed behavior of polystyrene latex spheres in spiral duct centrifuges are given in Figure 3. Families of theoretical curves are presented which correspond to the different operating conditions of the Stöber and Flachsbart (8) work. Calculations are done for two assumed flow conditions intended to envelope a most likely transitional flow profile. Agreement between theory and experiment is very good over a wide range of particle sizes and flow rates used in the studies, indicating that particle dynamics is being accurately simulated.

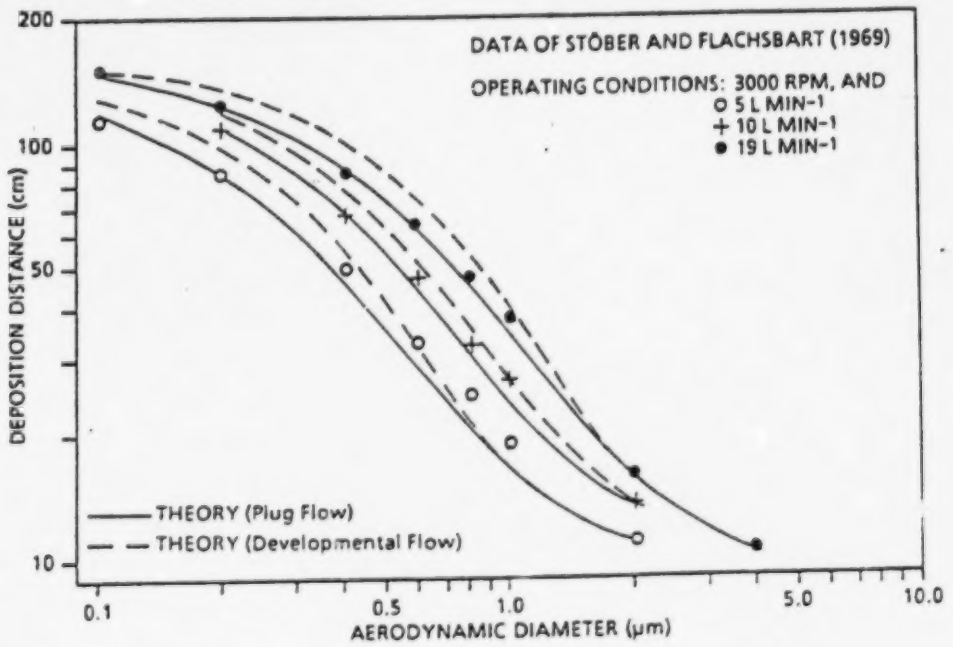

Figure 3. A comparison of theoretical and experimental calibration curves for a spiral duct centrifuge. The theoretical curves do account for secondary vortex flow currents.

Here, previous work is advanced by incorporating appropriate dynamic particle shape resistance factors into the theory, thereby extending it to nonspherical forms. Also, examples are provided of how centrifuge operating conditions may be selected a priori for aerodynamically characterizing fibrous aerosols.

3. Simulations of Airborne Fibers

In equation [1] there is a viscous drag term f_d expressing air resistance to motion. In the theory, any particular particle shape and orientation can be assumed by introducing appropriate drag force parameters into the derived trajectory equation.

For nonspherical orthotropic bodies a modified expression. $f'_d = 3\pi\mu D_g/K^*C(D_g)$, is introduced where K* is the representative dynamic shape resistance factor for settling particles undergoing rapid and random changes in orientation due to Brownian rotation. According to Happel and Brenner (1), K* may be written as the arithmetic average of translational shape resistance factors K_1, K_2, and K_3 corresponding to the three primary settling orientations of the particle. Fibers having no preferential airborne orientation and movement are simulated as this is anticipated to be the most general condition of motion. To simulate kinetics in an aerosol centrifuge a fiber with a circular cross-section of diameter D will be treated. In this case, $K_1 = K_2$. The appropriate factors for a fiber with length exceeding diameter may be approximated by the formulas

$$K_1 = K_2 = \frac{3\ D_{eq}\ (\text{LOG}\ 2\phi + 0.5)}{4D\phi} \qquad [2]$$

and

$$K_3 = \frac{3\ D_{eq}\ (\log 2\phi - 0.5)}{2D\phi} \qquad [3]$$

where D_{eq} is the equivalent volume diameter, and ϕ is the fiber aspect ratio, L/D. Factors K_1 and K_2 correspond to particle settling with the longitudinal axis perpendicular to the direction of motion, and K_3 is associated with that axis aligned with, or parallel to, the direction of settling (See Figure 1).

I have assumed an aerosol composed of fibers having diameters varying from 0.25 to 1.0 μm and lengths from 5 to 25 μm, dimensions corresponding to asbestos. The fiber aspect ratios, therefore, were: $5 \leq \phi \leq 100$. In Table 1 the calculated deposition patterns of fibers along the collection foil are given for a winnowing flow rate of 20 $Lmin^{-1}$ and a rotor speed of 3000 rpm. The deposition sites of fibers of prescribed lengths are presented as functions of assumed diameters (i.e., in the identified rows), and, in like manner, the deposition locations of fibers of specified diameters as related to various lengths are given in the respective columns.

TABLE 1. Deposition distances of sampled fibers along the collection foil of a centrifugal spectrometer as functions of particle dimensions.

Fiber Length (μm)	Fiber Diameter (μm)				Row Range (cm)	Data Band, Δ (%)
	0.25	0.50	0.75	1.0		
5	45.9	23.5	14.9	10.8	35.1	76.0
10	42.5	20.6	12.7	9.2	35.3	78.3
15	40.9	19.0	11.7	8.3	32.6	79.7
20	39.9	18.3	11.1	8.0	31.9	79.9
25	38.9	17.7	10.9	7.7	31.2	80.2
Column Range (cm)	7.1	5.8	4.1	3.1		
Data Band, Δ (%)	15.4	24.5	27.4	28.7		

A sampled fiber of length 20 μm has deposition distances measured down the centrifuge spiral duct varying from 8.0 cm for a 1 μm-diameter fiber (ϕ = 20) to 39.9 cm for a thinner one of 0.25 μm (ϕ = 80). The collection sites for a fiber of 0.5 μm diameter decrease from 23.5 to 17.7 cm as fiber length increases from 5 to 25 μm, a change in associated aspect ratio, ϕ, from 10 to 50. The respective dispersion of data are indicated by variation-of-size resolution bands, labeled as Δ. The Data Bands are calculated for each fiber diameter and length by subtracting the computed minimum deposition distance from the appropriate column and row from the corresponding maximum (these distance ranges are listed appropriately for each column and row in the separate Panels), dividing by that maximum, and multiplying by 100. The magnitudes of Δ are measures of centrifuge performance as regards aerosol discrimination. Comparisons of the Δ values under the respective column-and-row Data Band headings clearly demonstrate that an individual fiber's aerodynamic size is more dependent on its corresponding geometric diameter than its physical length.

Effects of different rotor speeds were examined; for example, for a fiber of ϕ = L/D = 15/0.5 = 30 deposition distances decreased from 39.5 cm (1000 rpm) and 29.3 cm (2000 rpm) to 19.0 cm (3000 rpm) at 20 $Lmin^{-1}$. Doubling the rotation rate, therefore, yielded a relative 26% decrease in deposition distance. Flow rate effects were also pronounced: at 3000 rpm the fiber locations were 12.4 cm (10 $Lmin^{-1}$) and 16.1 cm (15 $Lmin^{-1}$) compared to 19 cm (20 $Lmin^{-1}$). Doubling the flow rate produced a relative 53% increase in deposition distance.

Due to the geometry of a centrifuge's aerosol sampling inlet section, there is some inherent discrete width of particle deposits on collection foils even for highly monodisperse laboratory calibration aerosols of spherical particles. This width of the deposit, Δ, is approximately 5 to 10 percent of the total deposition distance (Stöber and Flachsbart (8)). The size resolution factor, therefore, is deemed to be a reliable relative indicator of performance standard in the tests.

In the evaluation of projected performance the optimal conditions to use for fiber sampling were accepted to be those which produced, simultaneously, the greatest Δ values for both columns and rows of tabulated data similar to that given here. Then, for a given fiber diameter the range of lengths examined are distributed over the widest interval along the collection foil. Likewise, for each fiber length the position of deposition is the most sensitive function of its diameter. Based on extensive results, chosen centrifuge operating conditions of 10 $Lmin^{-1}$ and 3000 rpm are recommended for the described fibrous aerosols.

DISCLAIMER

This document has been reviewed in accordance with U.S. Environmental Protection Agency policy and approved for publication. Mention of trade names or commercial products does not constitute endorsement or recommendations for use.

5. REFERENCES

(1) Happel, J. and H. Brenner: Low Reynolds Number Hydrodynamics, Martinus Nijhoff Pub., Boston (1964).

(2) Harris, Jr., R.L. and D.A. Fraser: A Model for Deposition of Fibers in the Human Respiratory System. Am. Ind. Hyg. Assoc. J. 37:73-89 (1976).

(3) Johnson, D.L. and T.B. Martonen: Aerosol Characterization with Centrifugal Aerosol Spectrometers: Theory and Experiment. Am. Ind. Hyg. Assoc. J. 50:408-412 (1989).

(4) Martonen, T.B., W. Hofmann and I. Balásházy: Physical Factors Affecting Lung Deposition of Cigarette Smoke (with Syncarcinogenic Radon Progeny Effects) and Mineral Fiber Particulate Matter. pp. 159-181. In Biological Interaction of Inhaled Mineral Fibers and Cigarette Smoke. Ed. A.P. Wehner, Battelle Press, Columbus, OH (1989).

(5) Myojo, T.: Deposition of Fibrous Aerosols in Model Bifurcations. J. Aerosol Sci. 18:338-347 (1987).

(6) Spurny, K.R.: Measurement and Analysis of Chemically Changed Mineral Fibers after Experiments in Vitro and in Vivo. Environ. Health Perspec. 51:343-355 (1983).

(7) Stahlhofen, W., G. Rudolf and A.C. James: Intercomparison of Experimental Regional Aerosol Deposition Data. J. Aerosol Med. 2:285-308 (1989).

(8) Stöber, W. and H. Flaschbart: Size Separating Precipitation of Aerosols in a Spinning Spiral Duct. Environ. Sci. Technol. 3:1280-1296 (1969).